FLEXOGRAPHIC PRINTING – HIGH THROUGHPUT TECHNOLOGY FOR FINE LINE SEED LAYER PRINTING ON SILICON SOLAR CELLS

Andreas Lorenz[1], Andre Kalio[1], Gunter Tobias Hofmeister[1], Sebastian Nold[1], Lorenz Friedrich[1],
Achim Kraft[1], Jonas Bartsch[1], Dietmar Wolf[2], Martin Dreher[2], Florian Clement[1], Daniel Biro[1]
[1]Fraunhofer Institute for Solar Energy Systems ISE, Heidenhofstr. 2, 79110 Freiburg, Germany
[2]Deutschsprachiges Flexodruck-Technologiezentrum DFTA-TZ, Nobelstraße 10, 70569 Stuttgart, Germany
Phone: +49 761 4588 5299, email: andreas.lorenz@ise.fraunhofer.de

ABSTRACT: Within this work, seed layer grids for solar cell front side metallization were applied using flexographic printing which represents an innovative, high-throughput approach for solar cell front side metallization. Fine line seed layer contact grids with a silver consumption lower than 10 mg per cell could be realized on alkaline textured Czochralski-grown silicon wafers with an edge length of 156 mm. Subsequently, the seed layer has been reinforced with silver using light induced plating (LIP). In order to determine the optimum LIP process, three groups were plated with different amounts of silver deposition. The results were analyzed before and after plating regarding silver consumption, contact finger geometry and interruptions. Solar cell parameters were determined after plating. It was demonstrated, that a homogeneous front side seed layer metallization without interruptions down to a line width of 25 µm can be realized using flexographic printing. The best cell reached a conversion efficiency of 18 % after silver LIP which is comparable to standard screen printed cells on the used Si wafer material. Furthermore, an economic comparison was carried out to illustrate the potential of solar cell metallization using rotational printing methods with subsequent Ag-LIP or Ni/Cu/Ag-LIP compared to state-of-the-art screen printing technology.
KEYWORDS: Flexographic Printing, Metallization, Cost Reduction, Silicon Solar Cell, Seed and Plate

1 INTRODUCTION

Reducing costs per Watt peak is currently the predominant goal for the solar cell industry. Considering the manufacturing costs, metallization is a mayor material cost driver in the manufacturing process of crystalline silicon solar cells [1]. To date screen printing is still the standard technology for applying the metallization within the crystalline silicon solar cell industry. However, screen printing holds limitations in terms of throughput, realization of narrow contact fingers and transfer of small amounts of silver on textured silicon substrates. Among others, deposition of plated silver via light induced plating (LIP) on printed and fired seed layers is one approach to improve emitter contact as well as the conductivity of the front side metallization compared to screen printed contact grids [2]. Reinforcing the printed and fired seed layer with nickel as diffusion barrier, copper as cheaper and equally conductive alternative to silver and a silver capping layer (Ni/Cu/Ag) using LIP is an even more promising approach to reduce the cost of the front side metallization process [3]. Other possibilities to realize the capping layer are tin (Sn) or organic surface protection (OSP). Several novel approaches like inkjet [4] and Aerosol printing [5,6] have been investigated to realize seed layer front side grids. Yet none of these technologies has been leveraged to industrial production due to limited throughput rates and inadequate reliability of the process.

Flexographic printing, also referred to as flexography or flexo, offers a promising high-throughput alternative to state-of-the-art screen printing technology. The potential of flexography to transfer fine line seed layer contact grids with very fast printing velocity enables this technology to reduce the cost of solar cell front side metallization significantly. Although screen printing is also able to transfer seed layers using fine line meshes, flexographic printing entails a significant silver reduction due to reduced seed layer thickness and a significantly higher output rate. Furthermore, small contact fingers with better edge definition can be realized, which is favorable to reduce shading on the active cell area [7, 8].

Flexography is a rotational printing method, which is widely used in roll-to-roll package printing on corrugated cardboard, foils, paper and other substrates. Several publications have demonstrated, that flexography is well suited for printed electronics applications, such as carbon nanotubes on polycarbonate foils [9], printed organic field-effect-transistors (OFETs) [10] or polymer solarcells [11,12]. Previous studies on laboratory scale at Fraunhofer ISE together with TU Darmstadt showed, that solar cells with flexo printed front side seed layers and subsequent Ag-LIP feature conversion efficiency gains up to 0.7% absolute compared to screen printed reference samples [7]. Further investigations suggest that printability and resulting finger geometry are governed by the paste viscosity [8].

The present contribution carries these investigations further and demonstrates that flexography is feasible to transfer fine line seed layer front side grids on Czochralski-grown textured silicon solar cells with an edge length of 156 mm. A detailed cost calculation compares the cell costs per Watt peak (W_p) for solar cell metallization using rotational printing methods at different output rates and subsequent Ag-LIP or Ni/Cu/Ag-LIP with state-of-the-art screen-printed cell metallization.

2 FLEXOGRAPHIC PRINTING

Flexographic printing is a usually roll-to-roll based printing method utilizing flexible relief printing plates. A steel cylinder with a finely textured chromium or ceramic surface, referred to as anilox roller, transfers a specific amount of ink from the ink reservoir onto elevated areas of the printing plate. This characteristic amount of ink is specified as dip volume and is defined by the angle, volume and line screening of the engraved cells. The dip volume is denoted in ml/m². Excessive ink is removed by a doctor blade before the anilox roller wets the printing plate with a uniform layer thickness. Finally, the ink is transferred from the printing plate onto the substrate (Fig.1) [7,13].

Flexography is well suited for high quality printing on rough surfaces due to the flexibility of the printing plate. As the printing process requires only low printing pressure, flexography is also well applicable for fragile substrates like silicon wafers. Flexographic printing platforms are usually roll-to-roll based. In order to use this technology for the metallization of silicon solar cells, a new roll-to-wafer machine will be required (Fig. 1).
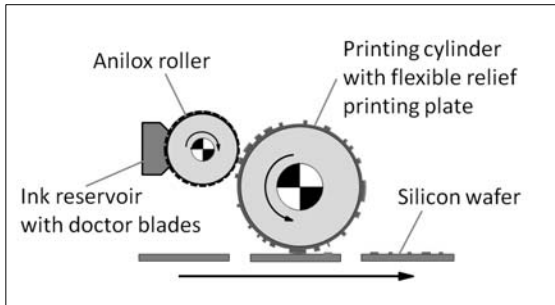

Figure 1: Flexographic printing: the ink is transferred by an anilox roller from the ink reservoir onto elevated elements of the printing plate and from there onto the silicon wafer

Other than screen printing pastes, which show a shear-thinning and thixotropic behavior with a yield point which has to be overcome to initiate the flow of the paste [20], inks used in flexographic printing typically show a very low viscosity and a negligible yield point. The effective viscosity of the ink during the printing process depends strongly on the shear stress within the printing nip. From literature, shear rates in the range of 1.000-100.000 s^{-1} [21] and viscosities between 50–500 mPas are stated as realistic for flexographic printing on industrial scale. Other sources assume a shear rate in the order of magnitude of 10.000 s^{-1} within the printing nip of flexographic printing machines [22]. The wide range of applicable shear rates can be explained by a variety of different rheological conditions during the printing process, as the ink has to pass from the ink reservoir over anilox roller and printing cylinder onto the substrate. Therefore, viscosity should be measured not only at one shear rate, but over a wider range of shear rates to extract a realistic prediction of the rheological behavior of the ink throughout the printing process.

3 EXPERIMENTAL APPROACH

3.1 Materials and printing platform

For the experiments, standard alkaline textured p-type Czochralski-grown silicon (Cz-Si) wafers with an edge length of 156 mm and an n-type emitter with a mean sheet resistivity of 65 Ω/sq and a base resistivity of 3-6 Ωcm were used. The wafer material has been coated with an antireflective layer on the front side. The back side metallization consisting of silver solder pads and aluminum back surface field (Al BSF) has been applied using standard screen printing technology and dried directly after printing in an inline furnace. An H-pattern grid design consisting of three busbars (1.5 mm width) and 84 contact fingers (25 µm width) has been designed for the front side metallization. A polymer printing plate with a shore hardness of 62° Shore A has been used as printing form. Using a high-resolution image setting

process, line widths of $w_f = 25$ µm have been generated on the printing form. As the mounting of the flat printing form on the round cylinder surface leads to an elongation of the resulting imprint, a length compensation within the digital data before the platemaking process has been carried out. To realize the front side seed layer metallization, a roll-to-plain flexographic printing machine with a vertically adjustable vacuum substrate holder has been used (Fig. 2). The printing form has been mounted onto the printing cylinder using an adequate substructure. The wafers were positioned manually on the substrate holder before each printing step.
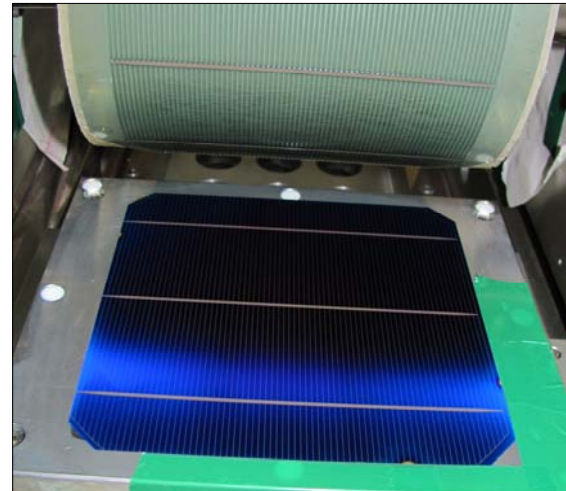

Figure 2: Flexographic printing platform used to carry out the roll-to-wafer printing experiments

A flexography seed layer ink has been prepared at Fraunhofer ISE (similar to the aerosol ink SISC [5,6,14]). The ink contains, besides solvents and dispersants for printability, particles smaller than 1 µm, namely silver and glass frit. The latter is responsible for contact formation and adhesion. Swell tests have been carried out to ensure the compatibility of the deployed solvent and the printing plate. Viscosity of the silver ink has been measured using an Anton Paar MCR 101 rotational rheometer with a cone-plate setup ($d_{cone} = 50$ mm, $\alpha = 1°$). The applied shear rate has been varied in a range of 0.001–10.000 s^{-1}.

3.2 Experimental setup

Printing experiments were conducted using flexographic printing at defined speed and printing pressure. An anilox roller with a screening of 130 l/cm has been used to transfer a defined amount of ink. The parameters of the printing process were kept constant over the complete cell batch to minimize influences of the printing process itself. The samples were subsequently dried for 2 minutes at T = 200°C using a cabinet drier. The amount of silver on the front side has been determined by weighing the cells before front side metallization and again after printing and contact firing. As the reference weighing before the flexo printed front side metallization includes organics within the dried back side metallization which have been burned out after the second measurement, the real amount of deposited silver on the front side could be slightly higher than the determined values. A firing variation at three peak set temperatures ($T_1 = 880°C$, $T_2 = 900°$, $T_3 = 920°C$) has been carried out in an industrial fast firing furnace to identify the optimum

contact firing conditions. Afterwards, the cells were fired at the optimum condition. Subsequent laser edge isolation on the back side has been carried out to ensure satisfying edge isolation for the LIP process. The contact width of the printed and fired contact fingers has been determined at two defined positions of each cell using an Olympus LEXT confocal microscope. The height of the seed layer contact fingers was measured at three positions at an ion polished representative cross-section using Hitachi SU-70 SEM. To evaluate the amount of interruptions within the printed and fired front side grid, a full-area scan in combination with an automatic detection of interruptions wider than the minimum pixel size of d_{min} = 21 µm has been carried out on representative cells before and again after plating.

Subsequently, the front side seed layer contacts were reinforced by Ag-LIP. To identify the optimum amount of deposited silver, three variations were carried out. The target amount of plated silver has been varied with 100 and 130 mg per cell using a standard inline plating process where the cells are fully immersed in the electrolyte during the process. An additional group has been plated with a target of 130 mg silver in a manual process where the cell is only wetted on the front side. This prevents the isolation between emitter and base from being shunted by parasitic plating at the laser groove. Subsequently, a second laser edge isolation has been carried out to reduce losses due to insufficient parallel resistance. Height and width of the plated contacts were again determined by confocal microscopy at identical positions. Contact resistance of representative samples was measured after plating using transfer length method (TLM) [17,18,19]. The best cell has been regenerated under illumination at an elevated temperature to avoid degradation by recombination-active boron-oxygen complexes [15,16]. Finally, the electrical solar cell parameters were quantified using an industrial cell tester (Fig. 3).
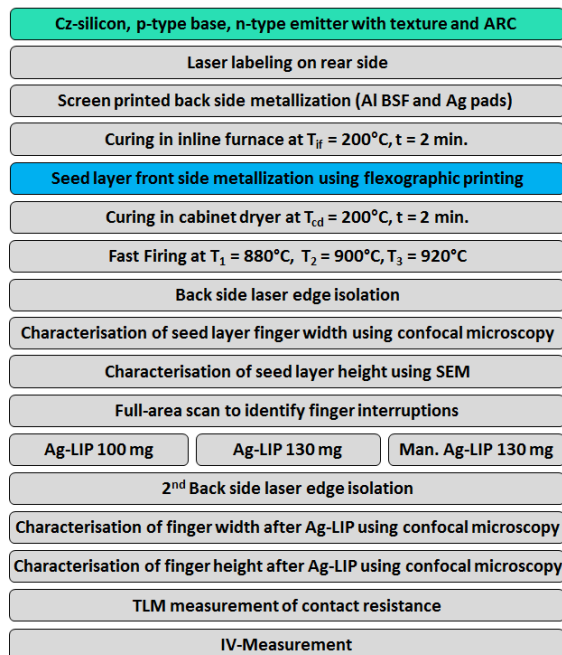
Cz-silicon, p-type base, n-type emitter with texture and ARC
Laser labeling on rear side
Screen printed back side metallization (Al BSF and Ag pads)
Curing in inline furnace at T_{if} = 200°C, t = 2 min.
Seed layer front side metallization using flexographic printing
Curing in cabinet dryer at T_{cd} = 200°C, t = 2 min.
Fast Firing at T_1 = 880°C, T_2 = 900°C, T_3 = 920°C
Back side laser edge isolation
Characterisation of seed layer finger width using confocal microscopy
Characterisation of seed layer height using SEM
Full-area scan to identify finger interruptions

Ag-LIP 100 mg	Ag-LIP 130 mg	Man. Ag-LIP 130 mg

2nd Back side laser edge isolation
Characterisation of finger width after Ag-LIP using confocal microscopy
Characterisation of finger height after Ag-LIP using confocal microscopy
TLM measurement of contact resistance
IV-Measurement

Figure 3: Experiment plan

4 EXPERIMENTAL RESULTS

4.1 Rheological investigations

As shown in figure 4, the silver ink which was prepared for the experiment shows a shear-thinning characteristic up to a shear rate of $\gamma \approx 500$ s^{-1} and approximates a near-Newtonian behavior at higher shear rates indicating that the viscosity stays constant at increasing shear rates $\gamma > 500$ s^{-1}. The result shows that the viscosity η_s = 50 mPa·s (at shear rate γ_s = 1.000 s^{-1}) of the prepared ink is within the typical range of flexographic inks.
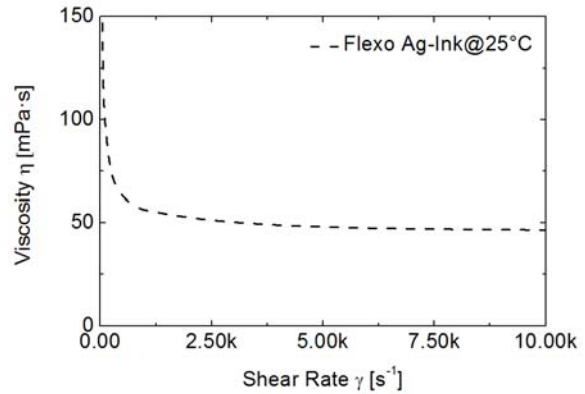

Figure 4: Dynamic viscosity of the silver ink

4.2 Analysis of silver deposition and finger geometry after flexographic printing and Ag-LIP

In spite of the relatively big dip volume of the anilox roller, a very low average amount of $m_{s,avg}$ = 9.5 mg silver after firing has been transferred on the front side of the cells via flexographic printing. The results of the full area scan of the front side grid revealed no significant interruptions wider than d_{min} = 21 µm on the selected cells after printing, which could lead to finger interruptions after Ag-LIP. Smaller interruptions are closed in most cases during LIP. In respect of the contact finger width, an average seed layer finger width w_s = 66.6 µm with a standard deviation of σ_s = 12.4 µm over all cells has been determined after contact firing. The smallest finger width was determined with $w_{s,min}$ = 24.7 µm (Fig. 5).

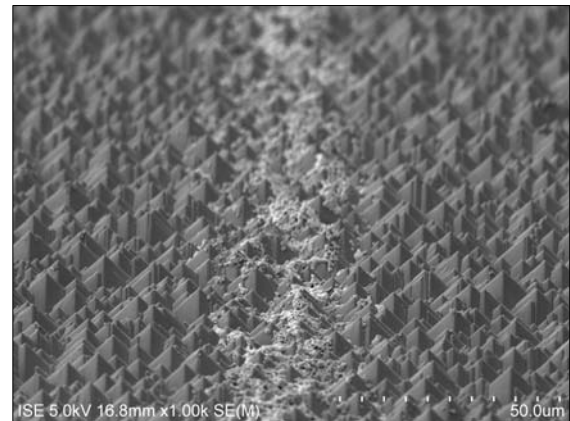**Figure 5:** Seed layer contact finger with finger width $w_{s,min}$ = 24.7 µm realized with flexographic printing

The average height of the printed and fired seed layer contacts is determined with $h_{s,avg}$ = 3.8 µm (standard deviation σ_h = 0,7 µm) at three positions of a cross-

section polish with SEM as shown in figure 6. The height was measured from the pyramid valleys.
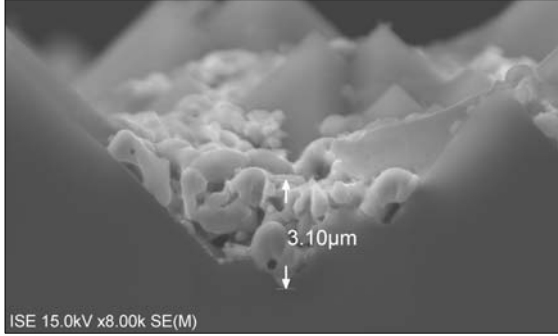

Figure 6: Determination of contact finger height via SEM

The printed and fired seed layer contacts were enhanced with Ag-LIP in three different variations. Variation A and B were enhanced using standard Ag-LIP process with an average silver deposition of $m_{A,avg} = 104.5$ and accordingly $m_{B,avg} = 135.7$ mg. Variation C has been processed using a one-side manual Ag-LIP with an average deposition of $m_{C,avg} = 130.5$ mg silver. Table I shows the resulting average finger width and height after Ag-LIP. Variation A showed the smallest finger width $w_{p,A} = 78.9$ µm after Ag-LIP, which can be traced back to the smallest initial seed layer width $w_{s,A} = 45.9$ µm on the one hand and a smaller amount of silver deposition by Ag-LIP on the other hand. Comparable finger widths $w_{p,B}$ and $w_{p,C}$ were determined for variation B and C, with slight differences resulting from varying initial seed layer widths w_s.

Table I: Finger geometry after printing and Ag-LIP

	∅ Seed layer width w_s [µm]	∅ Plated finger width w_p [µm]	∅ Plated finger height h_p [µm]
Var. A	45.9	78.9	10.4
Var. B	74.1	90.7	9.4
Var. C	64.5	84.8	8.4

4.3 Solar cell results

The printed and fired seed layers could be enhanced by Ag-LIP without difficulties and showed acceptable solar cell results (Table II). Taking a closer look at the solar cell parameters, it can be seen that the open circuit voltage V_{oc} shows typical values considering the used Si wafer material. As generally known, the cell current is increasing with reduced shading on the front side due to a higher amount of generated charge carriers. Thus, a smaller contact finger width w_p leads to an increased short circuit current density j_{sc}. As expected, a higher j_{sc} could be observed for cells of variation A with the smallest amount of silver deposition and thus the smallest average finger width w_p after plating. In order to evaluate the quality of the front side metallization, a closer look at the solar cell parameters related to the front side metallization is essential (Table III). Serial resistances $R_s < 1$ Ωcm² were determined on all variations after Ag-LIP. The comparison of the average grid resistance revealed, that variant B and C held a significantly lower grid resistance than variant A due to a the higher amount of plated silver on the front side contacts. As the fill factor *FF* shows no negative influence in consequence of the increased grid resistance, a deposition of 100 mg Ag or less by LIP is sufficient for

further experiments. The specific contact resistance ρ_c in the range of 6-8 mΩ·cm² is comparable to typical screen printed contacts. Parallel resistances $R_p > 1$ kΩcm² were determined on all plating variants. All three variants showed conversion efficiencies η, which are comparable to screen printing results on the used Si wafer material [23,24]. A detailed comparison of the conversion efficiency η showed a slightly enhanced average conversion efficiency η_A of variant A. This indicates that a lower amount of plated silver resulting in smaller finger width w_p after plating and thus a higher short circuit current density j_{sc} due to reduced shading is favourable for further experiments. A maximum conversion efficiency of $\eta_{max} = 18.0$ % after regeneration could be achieved in a following experiment with a slightly improved ink formulation, using the same process and material.

Table II: Solar cell results (as processed) after Ag-LIP measured with an industrial cell tester

		V_{oc} [mV]	J_{sc} [mA/cm²]	FF [%]	η [%]
Var. A	Avg.	625.9	36.8	77.1	17.8
	Best	625.9	36.7	77.4	17.8
Var. B	Avg.	625.5	36.5	77.3	17.6
	Best	626.2	36.6	77.9	17.8
Var. C	Avg.	626.7	36.5	76.9	17.6
	Best	625.7	36.5	77.4	17.7

Table III: Solar cell parameters related to the front side metallization after Ag-LIP

		GridRes [Ω/m]	R_s [Ωcm²]	ρ_c [mΩ·cm²]
Var. A	Avg.	53.3	0.8	5.9
Var. B	Avg.	37.7	0.7	6.4
Var. C	Avg.	36.1	0.8	8.2

5 ECONOMIC ANALYSIS AND COMPARISON

5.1 Input data for the cost calculation

A detailed economic comparison of solar cell metallization using rotational printing methods with state-of-the-art screen printing process was carried out using the Cost of Ownership calculation tool "SCost", which is developed at Fraunhofer ISE and enables a complete simulation of the whole value chain from the as-cut wafer to the finished PV module [25]. As the quality of the input data is essential for a realistic result of an economic analysis, data for this comparison is based on experience within the industrial scale pilot line at the Photovoltaic Technology Evaluation Center PV-TEC [26] as well as through the exchange with a wide range of industrial manufacturers.

To compare the economic potential of flexographic cell metallization with subsequent Ag-LIP or Ni/Ag/Cu-LIP with state-of-the-art screen printing, a virtual solar cell manufacturing plant with an estimated output of 1.2 GW_p/a has been taken as basis. An average conversion efficiency of $\eta_{avg} = 18.5$ % of the manufactured cells has been assumed for all process routes. Latest market prices for silicon wafer material, raw materials and supplies have been used. The resulting cell costs per W_p (Watt peak) were calculated for rotational cell metalli-

zation with subsequent Ag-LIP or Ni/Cu/Ag-LIP at variable output rates. The assumed output rate of the rotational cell metallization was varied between 1.000 and 10.000 Wafer/h. It was assumed, that not only the front side metallization but also the complete metallization on the back side (Ag pads and Al BSF) could be realized with rotational printing methods at the same output rate. An applied silver ink quantity of 10 mg for the seed layer metallization on the front side was assumed. For the subsequent plating step, an amount of 90 mg Ag and – in case of Ni/Cu/Ag-LIP – 9 mg Ni, 80 mg Cu and 2.5 mg Ag as capping layer was taken as basis in order to achieve a comparable conductivity. As reference, the resulting cell cost per W_p for a state-of-the-art screen printing process with an output rate of 1.800 Wafer/h and an applied quantity of 110 mg silver paste for the front side metallization was calculated and compared to the cell metallization based on rotational printing with Ag-LIP or Ni/Cu/Ag-LIP (Fig. 7).
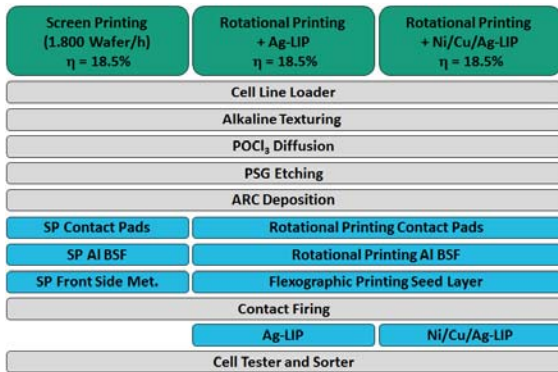

Figure 7: Comparison of cell manufacturing process routes using rotational printing with Ag- or Ni/Cu/Ag-LIP with a state-of-the-art cell manufacturing process using screen printing for front and back side metallization

5.2 Results of the economic comparison

For the reference process using state-of-the-art screen printing, the costs per cell (including wafer costs) were calculated with c_{sp} = 33.53 €ct/W$_p$. Using rotational printing methods with subsequent Ag-LIP, the output rate has to exceed at least 2.500 Wafer/h to compete with a state-of-the-art screen printing metallization. If the output rate of this cell metallization process could be increased to 5.000 Wafer/h, the cell costs per W_p can be lowered by 0.70 €ct/W$_p$ (2.1 %) compared to screen printing metallization. Increasing the output rate to 10.000 Wafer/h would lead to a cost saving potential of 0.98 €ct/W$_p$ (2.9 %), but such an output rate does not seem realistic. Looking at the cost saving potential of a cell metallization based on rotational printing with subsequent Ni/Cu/Ag-LIP, the economic advantage is much higher. Assuming the same output rate as state-of-the-art screen printing with 1.800 Wafer/h would already lead to a cost saving potential of considerable 0.54 €ct/W$_p$ (1.6 %) for a metallization based on this process. If the output rate could be increased to 5.000 Wafer/h, the cost saving potential can be raised to 1.66 €ct/W$_p$ (4.9 %) and 1.94 €ct/W$_p$ (5.8 %), if 10.000 Wafer/h could be realized. The comparison reveals further, that a higher output rate of the individual metallization lines lead to a significantly reduced number of required printing lines in total, thus the fixed costs for the metallization process decrease with increasing output rate. The variable costs on the other

hand, particularly material costs, stay constant with increasing output rate. This leads to a saturation of the cost curve at a certain level with increasing output rates, meaning that further increase of the output rate does not lead to a significant further reduction of the cell costs (Fig. 8).
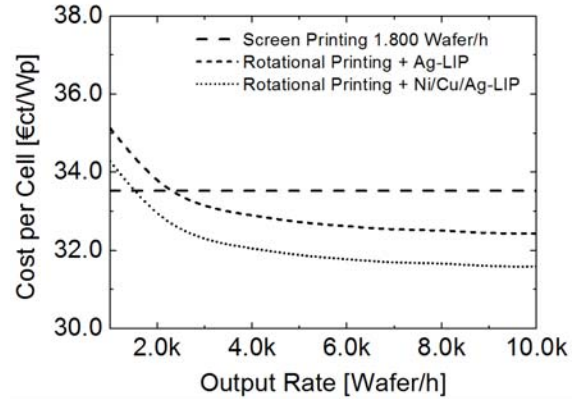

Figure 8: Comparison of cell costs (per W$_p$) for rotational printing with subsequent Ag-LIP or Ni/Cu/Ag-LIP cell metallization at variable output rates with state-of-the-art screen printing at an output rate of 1.800 Wafer/h

A detailed breakdown of the costs for front and back side metallization reveals, that a manufacturing process based on rotational printing with an output rate of 5.000 Wafer/h and subsequent Ag-LIP leads to a cost reduction of 12.5 % (0.70 €ct/W$_p$) compared to screen printing. A close investigation shows, that this can be traced back to the significantly increased output rate and thus reduction of the fixed costs of the rotational seed layer metallization on the one hand and to additional costs for parts (screen, squeegee) within the screen printing process on the other hand. In case of a cell metallization based on rotational printing with an output rate of 5.000 Wafer/h and subsequent Ni/Cu/Ag-LIP, the cost saving potential for metallization can even be raised to 29.5 % (1.66 €ct/W$_p$). Increased costs for equipment, utilities (electricity, cooling water, exhaust), waste disposal and yield loss of the additional LIP line with three required plating steps are excelled by significantly lower costs for process consumables (Ni and Cu plating solutions) leading to a considerable overall cost saving potential (Fig. 9).
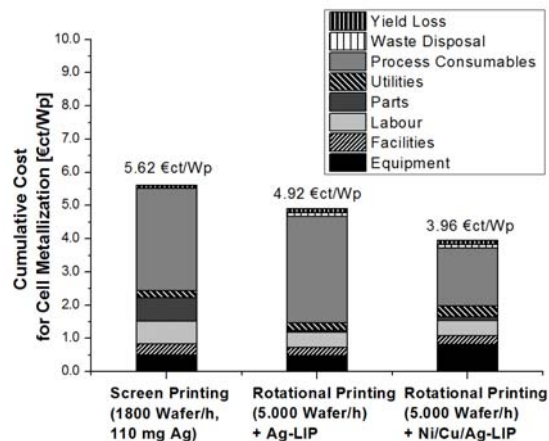

Figure 9: Detailed comparison of the cumulative costs for front and back side metallization using screen printing or rotational printing with Ag- or Ni/Cu/Ag-LIP

6 CONCLUSION

Within the present contribution, flexographic printing was applied on Czochralski-grown silicon wafers with an edge length of 156 mm to realize a seed layer front side metallization. A seed layer silver ink with a viscosity of $\eta_s = 50$ mPa·s at a shear rate of $\gamma_s = 1.000$ s^{-1} was prepared. Using this technology, a homogenous seed layer front side metallization with line widths down to $w_{s,min} = 24.7$ µm could be realized. A very low silver consumption $m_{s,avg} < 10$ mg per cell was determined for the seed layer. The printed and fired seed layer front contacts could be reinforced by Ag-LIP without problems. The amount of silver deposition within Ag-LIP was varied to identify the optimum amount of plated silver which could be determined with 100 mg. A maximum conversion efficiency of $\eta_{max} = 18.0$ % after Ag-LIP and regeneration could be reached on the best cell, which is in the range of expectation for the used Si wafer material.

Previous investigations indicate a high potential for flexographic printing to realize considerably smaller average printing widths with an enhanced homogeneity by further optimization of ink, printing form, anilox roller and machine adjustment. Further investigations should be carried out in order to identify the optimum process parameters for flexographic printing on silicon solar cells.

An economical comparison between rotational front and back side metallization at different output rates with subsequent Ag-LIP or Ni/Cu/Ag-LIP and standard Al BSF solar cells with state-of-the-art screen printed front and back side metallization was carried out. It was demonstrated, that the costs per cell can be decreased by 2.1 % (0.70 €ct/W$_p$) using rotational printing methods at an output rate of 5.000 Wafer/h and Ag-LIP. Using this process at the same output rate with subsequent Ni/Cu/Ag-LIP leads to a considerable cell cost reduction of 4.9 % (1.66 €ct/W$_p$). As a further increase of the output rate does not lead to a further significant cost reduction, a rotational printing system with a manufacturing output of approximately 4.000 - 5.000 Wafer/h is economically favourable. This shows that a rotational front and back side metallization is particularly attractive in combination with subsequent Ni/Cu/Ag-LIP. An even higher economic advantage can be expected, if the front side metallization could be realized using flexographic printing or other rotational printing methods without subsequent Ag- or Ni/Cu/Ag-LIP. A promising approach to achieve this might be multiple successive printing steps.

7 ACKNOLEDGEMENTS

8 REFERENCES

[1] Fischer, M. et al., *Semi international technology roadmap for photovoltaics (itrpv) challenges in c-si technology for suppliers and manufacturers*. Proc. of the 27th EU PVSEC (2012), Frankfurt, Germany

[2] Pysch, D. et al.,*Comprehensive analysis of advanced solar cell contacts consisting of fine-line seed layers thickened by silver plating*, Prog. Photovolt.: Res. Appl., Vol. 17, pp. 101–114.

[3] Bartsch, J. et al., *Progress with multi-step metallization processes featuring copper as conducting layer at Fraunhofer ISE*, Proc. of the 27th EU PVSEC (2012), Frankfurt, Germany, pp. 604–608.

[4] Ebong, A. et al., *Successful implementation of narrow Ag gridlines with inkjet machine for high quality contacts to silicon solar cells*, Proc. of the 26th EU PVSEC (2011), Hamburg, Germany, pp. 1711–1714.

[5] Mette, A. et al., Metal aerosol jet printing for solar cell metallization, Progr. Photovolt., 115 (2007), pp. 621-627.

[6] Hörteis, M. et al., *Further progress in metal aerosol jet printing for front side metallization of silicon solar cells*, Proc. of the 22nd EU PVSEC (2007), Milan, Italy, pp. 1039–1042.

[7] Frey, M. et al. *Frontside Metalization By Means Of Flexographic Printing*, Energy Procedia 8 (2011), pp. 581–586

[8] Thibert, S. et al. *Silver ink experiments for silicon solar cell metallization by flexographic process*, Proceeding of the 27th IEEE PVSC (2012), Austin, USA, pp. 2266- 2270

[9] Fischer, T. et al. *Flexographic Printed Carbon Nanotubes on Polycarbonate Films Yielding High Heating Rates*, Journal of Applied Polymer Science (2013), No. 1, pp. 1-9

[10] Schmidt, G. et al. *Fully mass printed organic field effect transistors with a transit frequency in the kHz range*, Proc. of the LOPE-C 2012. München, Germany, pp. 151-153

[11] Krebs, F. et al. *Product integration of compact roll-to-roll processed polymer solar cell modules: methods and manufacture using flexographic printing, slot-die coating and rotary screen printing*, Journal of Materials Chemistry (2010), No. 20, pp. 8994–9001

[12] Yu, JS et al. *Silver front electrode grids for ITO-free all printed polymer solar cells with embedded and raised topographies, prepared by thermal imprint, flexographic and inkjet roll-to-roll processes*, Nanoscale (2012), No. 19, pp. 6032-6040

[13] Kipphan, H., *Handbook of print media*, Heidelberg, Springer, (2000). pp. 416.

[14] Kalio, A. et al., *Metallization of n-type silicon solar cells using fine-line printing techniques*, Energy Procedia Vol. 8 (2011), pp. 571–576

[15] Herguth, A. et al. *Avoiding Boron-Oxygen related degradation in highly boron doped Cz Silion*, Proc. of the 21st EU PVSEC, Dresden, Germany (2006), pp. 530-537

[16] Herguth, A. et al. Further investigations on the avoidance of boron-oxygen related degradation by means of regeneration, Proc. of the 22nd EU PVSEC, Milan, Italy (2007), pp. 892-896

[17] Shockley, W., *Research and investigation of inverse epitaxial UHF power transistors*, Report No. Al-TOR-64-20 (1964), Air Force atomic laboratory, Wright-Patterson Air Force Base, Ohio (1964)

[18] Berger, H., *Contact Resistance and Contact Resistivity* J. Electrochem. Soc. Solid State Science and Technology Vol. 119, No. 4 (1972), pp. 507-514

[19] Murrmann, H. et al.: *Current crowding on metal contacts to planar devices*, IEEE Transactions on

Electron Devices 16 (1969), pp.1022-1024.

[20] Pospischil, M. et al. *Investigation of thick-film-paste rheology for dispensing appplications*, Proc. of the 1st international Conference on Silicon Photovoltaics, Freiburg, Germany (2011), pp. 449-454

[21] Barnes, H. et al., *An Introduction to Rheology*, Elsevier 7. Ed. (1989), pp. 199

[22] Kalpathy, S. et al., *Shear-induced suppression of rupture in two-layer thin liquid films*, Department of Chemical Engineering and Materials Science, University of Minnesota, Presented at the 15th International Coating Science and Technology Symposium, St. Paul, Minnesota (2010)

[23] Specht, J. et al., *High aspect ratio front contacts by single step dispensing of metal pastes*, Proc. of the 25th EU PVSEC, Valencia, Spain (2010), pp. 1867-1870

[24] Pospischil, M. et al., *Correlations between finger geometry and dispensing paste rheology*, Proc. of the 27th EU PVSEC, Frankuft, Germany (2012), pp. 1773-1776

[25] Nold, S. et al. *Cost Modeling of Silicon Solar Cell production innovation along the PV value chain*, Proc. of the 27th EU PVSEC (2012) Frankfurt, Germany, pp. 1084-1090

[26] Biro, D. et al. *PV-Tec: Photovoltaic technology evaluation center - design and implementation of a production research unit*, Proc. of the 21st EU PVSEC (2006) Dresden, Germany